

# Frequency dependence of lung volume changes during superimposed high-frequency jet ventilation and high-frequency jet ventilation

R. Sütterlin<sup>1\*</sup>, R. Priori<sup>2</sup>, A. Larsson<sup>1</sup>, A. LoMauro<sup>2</sup>, P. Frykholm<sup>1</sup> and A. Aliverti<sup>2</sup>

<sup>1</sup> Hedenstierna Laboratory, Anaesthesiology and Intensive Care, Department of Surgical Sciences, Uppsala University, Uppsala, Sweden

<sup>2</sup> Dipartimento di Elettronica, Informazione e Bioingegneria, Politecnico di Milano, Milan, Italy

\* Corresponding author. E-mail: robert.sutterlin@surgsci.uu.se

**Background.** Superimposed high-frequency jet ventilation (SHFJV) has proved to be safe and effective in clinical practice. However, it is unclear which frequency range optimizes ventilation and gas exchange. The aim of this study was to systematically compare high-frequency jet ventilation (HFJV) with SHFJV by assessing chest wall volume variations ( $\Delta\text{EEV}_{\text{CW}}$ ) and gas exchange in relation to variable high frequency.

**Methods.** SHFJV or HFJV were used alternatively to ventilate the lungs of 10 anaesthetized pigs (21–25 kg). The low-frequency component was kept at  $16 \text{ min}^{-1}$  in SHFJV. In both modes, high frequencies ranging from 100 to  $1000 \text{ min}^{-1}$  were applied in random order and ventilation was maintained for 5 min in all modalities. Chest wall volume variations were obtained using opto-electronic plethysmography. Airway pressures and arterial blood gases were measured repeatedly.

**Results.** SHFJV increased  $\Delta\text{EEV}_{\text{CW}}$  compared with HFJV; the difference ranged from 43 to 68 ml. Tidal volume ( $V_T$ ) was always  $>240$  ml during SHFJV whereas during HFJV ranged from 92 ml at the ventilation frequency of  $100 \text{ min}^{-1}$  to negligible values at frequencies  $>300 \text{ min}^{-1}$ . We observed similar patterns for  $P_{\text{aO}_2}$  and  $P_{\text{aCO}_2}$ . SHFJV provided generally higher, frequency-independent oxygenation ( $P_{\text{aO}_2}$  at least 32.0 kPa) and  $\text{CO}_2$  removal ( $P_{\text{aCO}_2} \sim 5.5$  kPa), whereas HFJV led to hypoxia and hypercarbia at higher rates ( $P_{\text{aO}_2} < 10$  kPa and  $P_{\text{aCO}_2} > 10$  kPa at  $f_{\text{HF}} > 300 \text{ min}^{-1}$ ).

**Conclusions.** In a porcine model, SHFJV was more effective in increasing end-expiratory volume than single-frequency HFJV, but both modes may provide adequate ventilation in the absence of airway obstruction and respiratory disease, except for HFJV at frequencies  $\geq 300 \text{ min}^{-1}$ .

**Keywords:** high-frequency jet ventilation; pulmonary ventilation; respiration, artificial

Accepted for publication: 10 May 2013

High-frequency jet ventilation (HFJV) has been used since the 1960s for a variety of procedures.<sup>1–5</sup> In patients with pulmonary disease or a significant degree of airway obstruction, carbon dioxide accumulation may occur, although it can be counteracted by increasing working pressure and thereby minute ventilation.<sup>6,7</sup> Higher driving pressures may however lead to increased air trapping when the airway is obstructed iatrogenically.<sup>8</sup> Although damage to the healthy lung by this distension is unlikely, there may be an increased risk of barotrauma in diseased lungs. To address the problem of  $\text{CO}_2$  elimination, superimposed HFJV (SHFJV) has been developed, a technique that combines normal frequency jet ventilation ( $12–20 \text{ min}^{-1}$ ) with jet ventilation at very high frequencies

(commonly  $>500 \text{ min}^{-1}$ ).<sup>9</sup> This method increases minute ventilation and facilitates carbon dioxide removal.<sup>10</sup> It may also increase end-expiratory lung volume (EELV), improving oxygenation.<sup>11</sup> The proposed mechanism is a PEEP effect by the superimposed high-frequency jet component, although this has not been proved in human or animal studies. Ventilation is usually delivered to the patient via two separate injector lines that are driven by one ventilator, allowing for separate adjustment of variables such as working pressure, inspiratory/expiratory ratio (*I/E* ratio), and frequency.

An important problem for the evaluation of jet ventilation is that there are no bedside techniques available for measurement of end-expiratory volume, tidal volume ( $V_T$ ), and minute

ventilation. The reason for the lack of volumetric techniques is that HFJV is usually applied in open systems in which air entrainment occurs to a varying extent, depending on the route of administration and the degree of airway obstruction,<sup>12–13</sup> and thus a pneumotachograph will not provide accurate values. Likewise, because of gas leakage and mixing with entrained gas, conventional inert gas methods are unsuitable for the assessment of EELV changes during jet ventilation.

Recently, opto-electronic plethysmography (OEP) has been developed for non-invasive measurements of chest wall volume changes.<sup>14</sup> OEP has been tested and validated in a variety of conditions and chest wall volume changes assessed by OEP correlate closely with changes in lung volume.<sup>15–18</sup> The technique provides a high enough temporal and spatial resolution to make it applicable for studies of jet ventilation.

One large study on patients with upper airway obstruction has shown that SHFJV provides effective ventilation during laryngoscopic or endoscopic airway surgery.<sup>19</sup> There are, however, no studies comparing SHFJV systematically with other modes of jet ventilation, neither are there any studies that examine which combination of frequencies is the most effective.

In the present study, we aimed to compare SHFJV with HFJV regarding end-expiratory chest wall (lung) volume ( $EEV_{CW}$ ),  $V_T$ , and gas exchange at several corresponding frequencies in a porcine model. Our hypothesis was that SHFJV would provide higher  $EEV_{CW}$  and  $V_T$  and thereby improve gas exchange compared with single-frequency jet ventilation at the same high frequency as used for SHFJV. Therefore, the aim of this study was to investigate the effect of increasing ventilation frequency on  $EEV_{CW}$  and  $V_T$ ,  $Pa_{O_2}$ , and  $Pa_{CO_2}$  using both SHFJV and HFJV modes. We chose a crossover design to increase power and limit the number of experimental animals used. The primary outcome variable was chest volume change and the secondary was gas exchange.

## Methods

Uppsala University Animal Research Ethics Committee approved the study and the National Institute of Health guidelines for animal research were followed.

### Anaesthesia and instrumentation

Ten pigs of ~3 months of age were included in the study. Exclusion criteria were obvious signs of disease (pyrexia, abnormal behaviour, signs of injury, or infection) and low baseline haemoglobin (because of the frequent blood sampling for gas analysis).

The animals (23–27 kg body weight) were premedicated by i.m. injections of xylazine 2.2 mg kg<sup>-1</sup>, tiletamine 3 mg kg<sup>-1</sup>, and zolazepam 3 mg kg<sup>-1</sup>. After ~10 min, the pigs were placed supine and vascular access was established by cannulation of an ear vein. After a bolus injection of fentanyl 100–500 µg i.v., tracheal intubation was performed. Subsequently, a surgical tracheotomy was performed under general anaesthesia and a cuffed tracheal tube (Hi-Contour™ Tracheal Tube, ID 8.0 mm, length cut to 210 mm, Mallinckrodt Medical, Athlone, Ireland) was inserted into the stoma. Volume control ventilation was started (Servo-I, Maquet, Sweden)

with  $V_T$  of 10 ml kg<sup>-1</sup> and the respiratory rate was adjusted to achieve normocarbia (5–6 kPa).

I.V. anaesthesia was started and maintained using i.v. pentobarbital (7–9 mg kg<sup>-1</sup> h<sup>-1</sup>) and morphine (420–540 µg kg<sup>-1</sup> h<sup>-1</sup>). After ascertaining that anaesthesia sufficiently prevented responses (signs of awakening or withdrawal reactions) to painful stimulation between the front toes, pancuronium (280–360 µg kg<sup>-1</sup> h<sup>-1</sup>) maintained neuromuscular block. Heart rate, arterial pressure, ECG,  $Sp_{O_2}$ , and signs of responsiveness to manipulations were monitored throughout the procedure.

Subsequently, the neck vessels were dissected and an arterial line for invasive arterial pressure measurement and blood gas sampling was placed in the left carotid artery. A pulmonary artery catheter was inserted into the left internal jugular vein and advanced into correct position verified by pressure monitoring.

Suprapubic urinary bladder catheterization was performed by a minilaparotomy and incision of the urinary bladder.

At the end of the experiment, the animals were euthanized under deep anaesthesia by an injection of potassium chloride.

## Interventions

Jet ventilation was administered with a Twinstream® jet ventilator (Carl Reiner GmbH, Vienna, Austria) by a Veres T-adaptor (Carl Reiner GmbH) through the cuffed tube inserted in the tracheostoma. Respiratory gas humidification was provided by a HumiCare® 200 breathing gas humidifier (Gründler medical GmbH, Freudenstadt, Germany) with a bias flow of 55 litre min<sup>-1</sup> (Fig. 1A and B).

The ventilator settings for the normal frequency component of ventilation were  $f=16$  min<sup>-1</sup>,  $I/E=1:1$ , and a working pressure of 1.6 bar. The high-frequency component had variable high frequencies ( $f_{HF}=100, 200, 300, 400, 500, 600, 800,$  and  $1000$  min<sup>-1</sup>), an  $I/E$  ratio of 1:1, and a working pressure of 0.8 bar were held constant for all of them. For SHFJV, both the low- and the high-frequency component were applied simultaneously. During HFJV, only the high-frequency component was used. NFJV involved the low-frequency component only.

The order of the high frequencies was randomized with a computer-generated method (Excel, Microsoft, Redmond, WA, USA). All high frequencies were tested twice in each pig; first during SHFJV (5 min) and thereafter in HFJV (5 min). In order to normalize chest wall and lung volume history, each frequency step (SHFJV–HFJV) was preceded by 5 min of normofrequent jet ventilation (NFJV, see Fig. 1B) followed by disconnection from the ventilator and 5 s apnoea. At each frequency, end-expiratory chest wall volume,  $V_T$ , and compliance were registered. Arterial blood gases were measured after 5 min of each ventilation step for immediate analyses of  $Pa_{O_2}$  and  $Pa_{CO_2}$  on a blood gas analyser (ABL 500, Radiometer, Copenhagen, Denmark).

The protocol was interrupted if systolic pulmonary artery pressure exceeded 60 mm Hg or when arrhythmias occurred during a hypoxic period, with NFJV or conventional ventilation using  $F_{I_{O_2}}$  1.0 as rescue management.

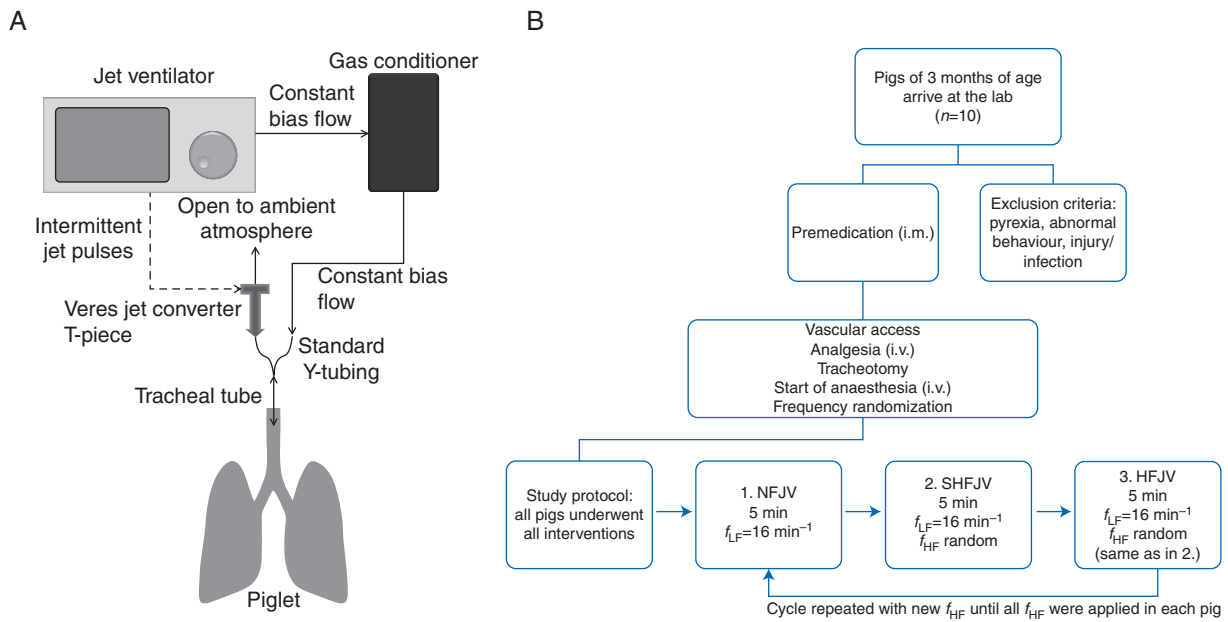


**Fig 1** Ventilator set-up (A) and flow scheme of the experimental protocol (B).

## Outcome measures

The primary outcome measure was changes in chest (lung) volume between SHFJV and HFJV at different frequencies. The secondary outcome measures were differences in  $Pa_{O_2}$  and  $Pa_{CO_2}$  between SHFJV and HFJV at different frequencies.

## Volume measurement

Chest wall volume was measured with OEP (Fig. 2). Using an OEP System<sup>®</sup> (BTS Bioengineering, Milan, Italy) consisting of six infra-red cameras, the position and movement of an array of 57 adhesive reflective markers on the pigs' chest wall was recorded.

Using the bundled OEP Capture<sup>®</sup> software (BTS Bioengineering), the position of each marker in a three-dimensional coordinate system was reconstructed for each time point (Fig. 1A). The volume enclosed by the surface formed by triangulation of the markers represents the chest wall volume. The method has been used in humans in a variety of conditions, corresponds well to lung volume changes and has high spatial and temporal resolution.<sup>14–18</sup> The standard deviation for repeated volume measurements that is attributable to OEP is  $<0.17\%$  ( $<1 \text{ ml}$  in our case).<sup>16</sup> The sampling frequency of the OEP system is 3.6 times higher than the highest frequency of the signal to be acquired. Therefore, according to the Nyquist–Shannon sampling theorem, the temporal resolution is sufficient for the study of high-frequency ventilation.

## Pressure registration

Tracheal airway pressure was monitored via a 200 mm long 16 G Secalon<sup>™</sup> Seldy catheter (BD Medical Surgical Systems, Stockholm, Sweden) at the tip of the tracheal tube. An

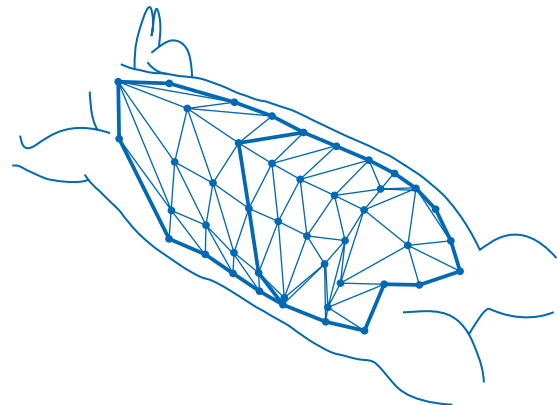


**Fig 2** Configuration of reflective markers on a pig's chest wall and the resulting geometrical model.

analogue pressure transducer (RCEM250DU, Sontortech GmbH, Puchheim, Germany) was used to acquire airway pressure readings that were recorded continuously and synchronized with the volume measurements by the OEP Capture<sup>®</sup> software (BTS Bioengineering).

## Data processing and definitions

As OEP measures total chest wall volume, not lung volume, it was necessary to define a reference volume in order to deduct changes in end-expiratory chest wall volume ( $\Delta EEV_{CW}$ ) and  $V_T$ . We chose end-expiratory chest wall volume during NFJV as reference volume. At an NFJV frequency as

low as  $16 \text{ min}^{-1}$ , the duration of the expiratory phase is 1.9 s and thus, almost complete expiration occurs because of the open ventilation system. Therefore,  $EEV_{CW}$  during NFJV is approximately equal to apnoeic functional residual capacity (FRC).

The calculation of  $\Delta EEV_{CW}$  was performed for every pig for each frequency step to compensate for potential changes in total chest wall volume over time that could be caused by, for example, fluid redistribution or accumulation because of the long total duration of the experiment.

All volumes and pressures derived from the raw data represent the mean values of at least five consecutive steady-state breaths.

We defined changes in end-expiratory chest wall volume ( $\Delta EEV_{CW}$ ) as follows:

$$\Delta EEV_{CW_{SHFJV}} = EEV_{CW_{SHFJV}} - EEV_{CW_{NFJV}}$$

and

$$\Delta EEV_{CW_{HFJV}} = EEV_{CW_{HFJV}} - EEV_{CW_{NFJV}}$$

$V_T$  was defined as the difference between end-inspiratory ( $EIV_{CW}$ ) and end-expiratory chest wall volume as follows:

$$V_T = EIV_{CW} - EEV_{CW}$$

PEEP was defined as the pressure registered at end-expiration. Pressure over PEEP was consequently calculated as follows:

$$\text{Pressure over PEEP} = \text{Peak inspiratory pressure} - \text{PEEP}$$

### Static and dynamic compliance

To control for changes in respiratory mechanics over the full duration of the experiment, static compliance measurements were performed at the beginning and end of the protocol, while dynamic compliance was measured at each frequency step of the protocol. To assess static compliance, an incremental–decremental PEEP manoeuvre was performed during pressure control ventilation: PEEP was increased by 2 cm H<sub>2</sub>O every 5 breaths, starting from 0 up to 20 cm H<sub>2</sub>O and successively decreased in the same manner until 0 cm H<sub>2</sub>O was reached. Using the pressure–volume curves (data not shown) derived from the PEEP values of each level and the corresponding end-expiratory chest wall volume as obtained by OEP, static compliance was calculated.

Dynamic compliance was assessed only during SHFJV (averaged from several consecutive breaths) as the oscillating maximum and minimum pressure and volume signals displayed a phase offset for all frequencies  $>100 \text{ min}^{-1}$  during HFJV.

### Statistical data analysis

Statistical computations were performed using the SigmaStat® (Systat Software, Inc., Chicago, IL, USA) and R (R Foundation for Statistical Computing, Vienna, Austria). Power calculations for the primary outcome variables  $EEV_{CW}$  and  $V_T$  were not attempted, as there were no data available on lung volume

differences between HFJV and SHFJV in direct comparisons. However, based on the assumption that a difference in the secondary outcome variables  $Pa_{CO_2}$  and  $Pa_{O_2}$  of at least 2 kPa with a standard deviation of 1.0 kPa would be clinically relevant, we performed a power calculation (analysis of variance, 8 frequency groups). For a  $P$ -value of  $<0.05$  with a power of at least 80%, at least nine animals would be needed. The final number of 10 pigs was chosen to compensate for the lack of power analysis for the primary outcome variables in order to increase the likelihood of significant findings also for the OEP volumes.

Our aim was to test the alternative hypothesis that SHFJV would provide higher  $EEV_{CW}$  and  $V_T$  and improve gas exchange compared with single-frequency jet ventilation at the same high frequency as used for SHFJV. Therefore, statistical analyses of  $\Delta EEV_{CW}$ ,  $V_T$ ,  $Pa_{O_2}$ , and  $Pa_{CO_2}$  were performed using linear mixed model analysis with pig ID as a random factor and mode (HFJV and SHFJV) and frequency and the interaction between mode and frequency as fixed factors. With pig ID as random factor, each pig was considered individually because of the repeated measurements. For all endpoints except  $\Delta EEV_{CW}$ , the dependent variable was log transformed before the analyses.

All data are presented as mean (or geometric mean for variables that were logarithmically transformed before analyses) and 95% confidence intervals (CIs). As the mixed model was used to characterize the properties of our observations, significant results should be interpreted as descriptive rather than confirmatory.

### Interpretation of the statistical analyses

In order to facilitate the interpretation of the results of the mixed model analyses, we subdivided the whole model and present here separate results for HFJV and SHFJV. Full details of the statistical analyses are provided in the Supplementary material.

The results allow for the calculation of predicted values for each outcome variable at different frequencies  $f_n$ . This can be done as follows:

$$EEV_{CW_{f_n}} = \text{Intercept} + n \times \text{Frequency}$$

$$V_{T_{f_n}} = \text{Intercept} \times \text{Frequency}^n$$

$$Pa_{O_{2f_n}} = \text{Intercept} \times \text{Frequency}^n$$

$$Pa_{CO_{2f_n}} = \text{Intercept} \times \text{Frequency}^n$$

where Intercept corresponds to the predicted value of the outcome variable at  $f_{HF}=0 \text{ min}^{-1}$  and  $n$  is the  $n$ th  $f_{HF}$  increase by  $100 \text{ min}^{-1}$  (e.g.  $n=1$  for  $f_{HF}=100$ ,  $n=2$  for  $f_{HF}=200 \text{ min}^{-1}$  and so forth).

As a result of the antilogarithmic transformation, the Frequency coefficient for each variable that was previously log transformed ( $V_T$ ,  $Pa_{O_2}$ ,  $Pa_{CO_2}$ ) describes a relative slope change per  $f_{HF}$  increase by  $100 \text{ min}^{-1}$ . For the same reason, the frequency estimates (Table 1) are stated without units.

**Table 1** Results from the mixed models analysis, partial analyses for HFJV and SHFJV. Whole model results are provided in Supplementary material. Intercept: predicted absolute value of the variable at  $f_{HF}=0 \text{ min}^{-1}$  ( $P<0.05$  indicates intercept significantly different from zero). Frequency: predicted change in slope per 100  $\text{min}^{-1}$  frequency increase ( $P<0.05$  indicates significant change when increasing  $f_{HF}$  by 100  $\text{min}^{-1}$ )

	Estimate	95% CI	P-value
<b>EEV<sub>CW</sub></b>			
HFJV			
Intercept (ml)	97.3	84.0–110.5	<0.00001
Frequency (ml per 100 $\text{min}^{-1}$ )	2.6	0.9–4.2	0.00332
SHFJV			
Intercept (ml)	164.9	146.1–183.7	<0.00001
Frequency (ml per 100 $\text{min}^{-1}$ )	–0.2	–1.9–1.5	0.8365
<b>V<sub>T</sub></b>			
HFJV			
Intercept (ml)	102.7	76.0–138.7	<0.00001
Frequency (times per 100 $\text{min}^{-1}$ )	0.597	0.566–0.629	<0.00001
SHFJV			
Intercept (ml)	289.1	264.3–316.2	<0.00001
Frequency (times per 100 $\text{min}^{-1}$ )	0.979	0.972–0.985	<0.00001
<b>Pa<sub>O<sub>2</sub></sub></b>			
HFJV			
Intercept (kPa)	35.8	26.4–48.4	<0.00001
Frequency (times per 100 $\text{min}^{-1}$ )	0.716	0.670–0.765	<0.00001
SHFJV			
Intercept (kPa)	34.2	32.0–36.6	<0.00001
Frequency (times per 100 $\text{min}^{-1}$ )	0.993	0.986–1.000	0.05103
<b>Pa<sub>CO<sub>2</sub></sub></b>			
HFJV			
Intercept (kPa)	6.2	4.9–7.8	<0.00001
Frequency (times per 100 $\text{min}^{-1}$ )	1.133	1.070–1.200	0.00024
SHFJV			
Intercept (kPa)	4.5	4.1–5.0	<0.00001
Frequency (times per 100 $\text{min}^{-1}$ )	1.022	1.013–1.031	0.00002

## Results

No animals were excluded from the study.

Observed values are presented in Table 2; the results from the mixed models analyses for  $\Delta\text{EEV}_{\text{CW}}$ ,  $V_{\text{T}}$ ,  $\text{Pa}_{\text{O}_2}$ , and  $\text{Pa}_{\text{CO}_2}$  are summarized in Table 1.

Airway pressures and haemodynamic data are detailed in the Supplementary material.

### End-expiratory volume

Superimposed HFJV increased  $\Delta\text{EEV}_{\text{CW}}$  compared with HFJV (Fig. 3A and Supplementary material). The difference was greatest at low ventilation rates—68 ml at  $f_{\text{HF}}=100 \text{ min}^{-1}$ . Whereas  $\Delta\text{EEV}_{\text{CW}}$  was fairly constant with SHFJV for all frequencies, we observed an increase in  $\Delta\text{EEV}_{\text{CW}}$  from 79 (95% CI: 58–99) ml at  $f_{\text{HF}}=100$  to a value of 116 (95% CI: 97–135) ml at  $f_{\text{HF}}=300 \text{ min}^{-1}$ , with  $\Delta\text{EEV}_{\text{CW}}$  remaining at about the latter level at higher ventilation frequencies [predicted slope of +2.6 (95% CI: 0.9–4.2) ml per 100  $\text{min}^{-1}$ ].

### Tidal volume

$V_{\text{T}}$  was also greater when SHFJV was used (Fig. 3B and Supplementary material)— $V_{\text{T}}$  levels were observed to remain  $>240$  ml, with a slight slope reduction of 0.979 (95% CI: 0.972–0.985) times per 100  $\text{min}^{-1}$  (i.e. a  $V_{\text{T}}$  reduction of 2.1% with every  $f_{\text{HF}}$  increase by 100  $\text{min}^{-1}$ ) revealed by the mixed model analysis.

Conversely, during HFJV,  $V_{\text{T}}$  was 92 (95% CI: 81–105) ml at  $f_{\text{HF}}=100 \text{ min}^{-1}$ , and decreased to very low values at rates  $>300 \text{ min}^{-1}$ . In the mixed model analysis, the frequency dependence of  $V_{\text{T}}$  during HFJV could be described by a slope decrease of 0.597 (95% CI: 0.566–0.629) times per 100  $\text{min}^{-1}$  (i.e. a 40.3%  $V_{\text{T}}$  reduction with every  $f_{\text{HF}}$  increase by 100  $\text{min}^{-1}$ ).

### Gas exchange

We observed a fairly constant  $\text{Pa}_{\text{O}_2}$  level of at least 32.0 (95% CI: 29.1–35.1) kPa during SHFJV throughout the range of studied frequencies (Fig. 4). Similarly, the observed  $\text{Pa}_{\text{CO}_2}$  during SHFJV remained at 5.5 (95% CI: 5.0–6.1) kPa. In contrast, while HFJV produced normal  $\text{Pa}_{\text{O}_2}$  levels at the two lowest

**Table 2** Observed values and model prediction. Values are arithmetic mean and 95% CI (EEV<sub>cw</sub>) and geometric mean with 95% CI (V<sub>T</sub>, Pa<sub>O<sub>2</sub></sub>, and Pa<sub>CO<sub>2</sub></sub>) for HFJV and SHFJV at each f<sub>HF</sub>. \*Significant (P<0.05) increase with increasing frequency (+2.6 ml per 100 min<sup>-1</sup>). †Significant (P<0.05) slope decrease with increasing frequency [0.597 times per 100 min<sup>-1</sup> (i.e. -40.3% per 100 min<sup>-1</sup>)]. ‡Significant (P<0.05) slope decrease with increasing frequency [0.979 times per 100 min<sup>-1</sup> (i.e. -2.1% per 100 min<sup>-1</sup>)]. §Significant (P<0.05) slope decrease with increasing frequency [0.716 times per 100 min<sup>-1</sup> (i.e. -28.4% per 100 min<sup>-1</sup>)]. ¶Significant (P<0.05) slope increase with increasing frequency [1.133 times per 100 min<sup>-1</sup> (i.e. +13.3% per 100 min<sup>-1</sup>)]. ††Significant (P<0.05) slope increase with increasing frequency [1.022 times per 100 min<sup>-1</sup> (i.e. +2.2% per 100 min<sup>-1</sup>)].

Variable	Mode	100 min <sup>-1</sup>	200 min <sup>-1</sup>	300 min <sup>-1</sup>	400 min <sup>-1</sup>	500 min <sup>-1</sup>	600 min <sup>-1</sup>	800 min <sup>-1</sup>	1000 min <sup>-1</sup>
EEV <sub>cw</sub> (ml)	HFJV*	78.6 (58.3–98.9)	103.8 (89.8–117.9)	116.4 (97.4–135.4)	115.4 (106.5–124.3)	116.5 (105.8–127.2)	113.3 (96.8–129.8)	115.4 (103.3–127.6)	116.3 (96.9–135.6)
	SHFJV	146.9 (119.4–174.4)	161.4 (135.7–187.0)	178.7 (155.5–201.8)	171.2 (161.3–181.2)	165.2 (148.1–182.2)	164.2 (142.1–186.2)	161.5 (142.1–180.9)	158.8 (141.3–176.3)
V <sub>T</sub> (ml)	HFJV†	92.4 (81.4–104.9)	39.8 (34.4–46.1)	26.8 (23.1–31.0)	15.0 (13.1–17.2)	3.5 (1.8–7.0)	2.7 (2.2–3.4)	1.5 (1.1–2.0)	1.1 (0.7–1.7)
	SHFJV‡	324.8 (300.2–351.3)	270.6 (250.4–292.5)	261.2 (238.8–285.6)	251.4 (231.6–272.9)	244.0 (227.9–261.2)	246.6 (221.5–274.7)	249.3 (223.1–278.5)	246.2 (224.0–270.6)
Pa <sub>O<sub>2</sub></sub> (kPa)	HFJV†	29.0 (21.1–40.0)	18.4 (13.8–24.5)	11.4 (8.1–16.1)	9.5 (6.6–13.6)	12.1 (NA)	8.3 (NA)	3.9 (2.2–6.8)	NA (NA)
	SHFJV	35.1 (32.3–38.2)	32.3 (29.7–35.1)	33.5 (31.5–35.7)	33.5 (31.4–35.8)	32.5 (30.0–35.2)	33.5 (31.4–35.7)	32.0 (29.1–35.1)	32.1 (29.4–35.0)
Pa <sub>CO<sub>2</sub></sub> (kPa)	HFJV§	5.5 (4.2–7.1)	9.1 (7.8–10.5)	10.7 (8.7–13.1)	10.0 (8.5–11.8)	8.0 (NA)	8.3 (NA)	10.3 (7.4–14.3)	NA (NA)
	SHFJV¶	4.3 (3.6–5.0)	5.0 (4.4–5.6)	4.8 (4.3–5.4)	5.2 (4.7–5.8)	5.2 (4.8–5.7)	5.1 (4.7–5.7)	5.4 (4.8–6.0)	5.5 (5.0–6.1)

studied frequencies [29.0 (95% CI: 21.1–40.0) kPa at f=100 min<sup>-1</sup>], rates >300 min<sup>-1</sup> were associated with hypoxia, in several animals of a degree that necessitated aborting the experiment prematurely. There was a concurrent increase in Pa<sub>CO<sub>2</sub></sub> from 5.5 (95% CI: 4.2–7.1) to 10.7 (95% CI: 8.7–13.1) kPa when increasing f<sub>HF</sub> from 100 to 300 min<sup>-1</sup>, after which missing data preclude meaningful descriptive statistics.

In the mixed model analysis of Pa<sub>O<sub>2</sub></sub> during SHFJV, there was no significant slope change over frequency. Conversely, for HFJV, increasing f<sub>HF</sub> by 100 min<sup>-1</sup> resulted in a slope reduction of 0.716 (95% CI: 0.670–0.765) times per 100 min<sup>-1</sup> (i.e. a decrease of Pa<sub>O<sub>2</sub></sub> by 28.4% for every f<sub>HF</sub> increase by 100 min<sup>-1</sup>). For Pa<sub>CO<sub>2</sub></sub>, the model predicts a slope change of 1.022 (95% CI: 1.013–1.031) times per 100 min<sup>-1</sup> for SHFJV (i.e. a 2.2% increase in Pa<sub>CO<sub>2</sub></sub> per 100 min<sup>-1</sup> f<sub>HF</sub> increase) and a change of 1.113 (95% CI: 1.070–1.200) times per 100 min<sup>-1</sup> for HFJV (i.e. a 13.3% increase in Pa<sub>CO<sub>2</sub></sub> per 100 min<sup>-1</sup> increase in f<sub>HF</sub>).

Because of missing data at very high frequencies, there is some uncertainty in the descriptive function of the frequency effect of the gas exchange variables.

## Airway pressures and dynamic compliance

Airway pressure results are available in the Supplementary material. Because of technical problems with the registration of intratracheal pressure, full dynamic compliance computations could only be performed in four pigs. Dynamic compliance during SHFJV was constant throughout the frequency span, with slight variations between 19.0 (18.4–20.6) and 21.2 (19.8–21.2) ml (cm H<sub>2</sub>O)<sup>-1</sup>.

## Discussion

The present study is the first to compare the influence of SHFJV and HFJV over a range of frequencies on lung volume and gas exchange *in vivo*. We found consistently higher values of ΔEEV<sub>cw</sub> and V<sub>T</sub> and improved gas exchange with SHFJV compared with HFJV.

Single-frequency HFJV resulted in an increase in end-expiratory chest wall volume above apnoeic FRC. For SHFJV, the increase in EEV<sub>cw</sub> was consistently higher than during HFJV with the same f<sub>HF</sub>, driving pressure, and I/E ratio settings on the ventilator. The frequency dependence of EEV<sub>cw</sub> during HFJV has been described earlier,<sup>20</sup> but there was a lack of similar data for SHFJV.

V<sub>T</sub> was highest in both modes at lower frequencies and decreased to stable plateau values at high frequencies, with SHFJV providing generally higher V<sub>T</sub> than HFJV, potentially caused by higher peak airway pressures (see Supplementary material). Similar findings have been reported in a study of HFJV.<sup>20</sup> The present study corroborates the findings from a previous study in patients where we found that SHFJV resulted in higher V<sub>T</sub> compared with single-frequency JV when the same route of application was chosen.<sup>21</sup>

Although many mechanisms of gas transport and gas mixing are known to influence gas exchange during pure high-frequency ventilation, at least part of the gas transport at lower frequencies

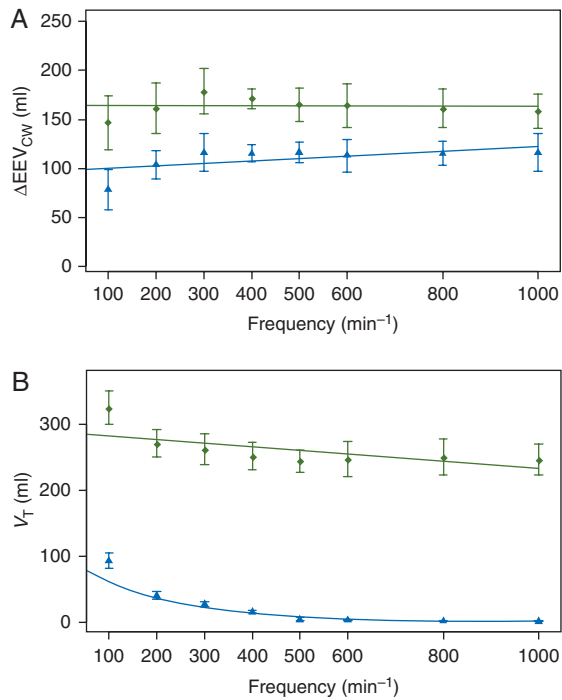


**Fig 3** Arithmetic mean and 95% CI for  $\Delta\text{EEV}_{\text{CW}}$  (A) and geometric mean with 95% CI for  $V_T$  (B) for SHFJV (green diamonds) and HFJV (blue triangles) with corresponding descriptive functions (green and blue lines for SHFJV and HFJV, respectively) derived from the mixed model analyses. For all frequencies, both  $\Delta\text{EEV}_{\text{CW}}$  and  $V_T$  during SHFJV were significantly higher than during HFJV ( $P < 0.05$ ).

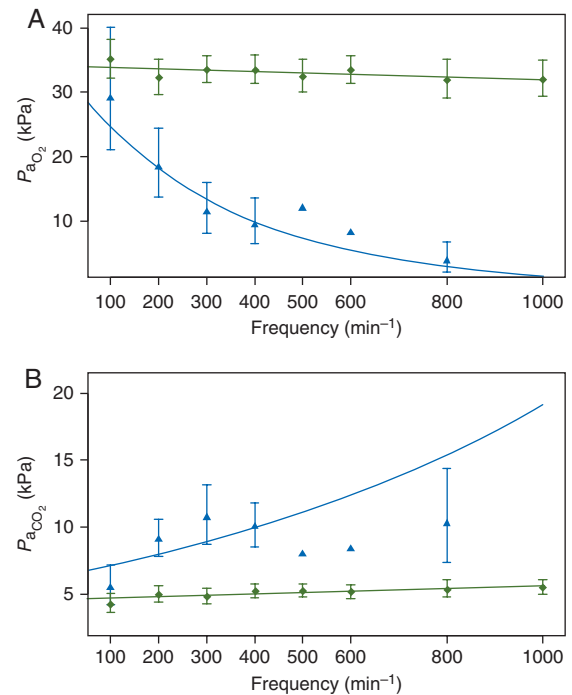


**Fig 4** Arterial partial pressures of oxygen (A) and carbon dioxide (B), indicated as geometric mean and 95% CI (green diamonds for SHFJV, blue triangles for HFJV) with corresponding function derived from the mixed model analyses (green and blue lines for SHFJV and HFJV, respectively). There was a clear influence of frequency on oxygenation during HFJV ( $P < 0.05$ ), whereas  $P_{\text{aO}_2}$  during SHFJV was practically independent of frequency.

can be explained by direct alveolar minute ventilation.<sup>22–25</sup> Indeed, it is known that gas exchange at very high rates of HFJV becomes insufficient,<sup>26–27</sup> with a breakpoint at  $\sim 300 \text{ min}^{-1}$ .<sup>28</sup> These findings are supported by our results, although we observed a more gradual decrease in  $P_{\text{aO}_2}$  and increase in  $P_{\text{aCO}_2}$  with increasing frequency. At frequencies  $> 300 \text{ min}^{-1}$ , however, ventilation was reduced to clinically unacceptable values. The severe reduction in  $P_{\text{aO}_2}$  already after 5 min at rates  $> 300 \text{ min}^{-1}$  might seem surprising, since apnoeic ventilation (without any ventilation at all) with an  $F_{\text{IO}_2}$  of 1.0 has been found to maintain adequate oxygenation for long periods.<sup>29</sup> However, when  $< 100\%$  oxygen is used during apnoeic oxygenation, nitrogen accumulation occurs quickly.<sup>30</sup> We used  $F_{\text{IO}_2}$  0.5 and therefore we believe that a similar mechanism explains the severe hypoxaemia found in our study. In addition, the high oxygen consumption in pigs may have accentuated this effect.

Our results indicate that during SHFJV, ventilation (i.e.  $\text{CO}_2$  removal) is mainly produced by the low frequency, whereas the increase in end-expiratory volume is produced by the superimposed HFJV (inducing gas trapping), and that changing the high frequency will have negligible influence on PEEP and the EELV (Fig. 3 and Supplementary Table S1). In fact, we found that  $\Delta\text{EEV}_{\text{CW}}$ ,  $V_T$ , minute ventilation, and  $P_{\text{aO}_2}$  and  $P_{\text{aCO}_2}$  were all practically constant over a wide range of frequency settings.

A limitation of the study is that we tested our hypotheses in a porcine model. The animals had lower lung volumes and thus lower lung and chest wall compliances than adult patients. The results should therefore be interpreted with caution and are not immediately transferable to patients, although porcine and human respiratory physiology are generally quite similar. Secondly, OEP measures chest wall volume rather than lung volume. Although it has been shown to correlate well with lung volume in humans, we did not investigate whether the changes represented further inflation of already aerated lung tissue or if recruitment or derecruitment of collapsed lung tissue occurred. Gas distribution and gas exchange during HFJV are complex and minute ventilation calculated by OEP chest wall volume cannot entirely reflect the actual movement of oxygen and carbon dioxide. Other mechanisms than bulk air movement are known to contribute to intrapulmonary gas distribution and gas exchange.<sup>31</sup> Thirdly, we used only 10 animals based on the assumption that the chest wall volume would behave in a similar way as  $P_{\text{aO}_2}$ . In fact, a *post hoc* test verified that 10 animals would give a  $\beta = 0.8$  with an  $\alpha = 0.05$ .

With intervention periods of only 5 min, conclusions on long-term effects of ventilation cannot be drawn. As the time constants for  $\text{EEV}_{\text{CW}}$  recruitment indicate, steady state for the increase in  $\text{EEV}_{\text{CW}}$  is reached within the time of observation.

Nevertheless, our results are likely to underestimate changes in ventilation efficacy after longer ventilation periods because the 5 min used in the present study might be too short to allow for equilibration of gases between the blood and the alveoli.

## Conclusion

In a porcine model without airway obstruction, we used OEP to show that SFHJV was more effective than single-frequency HFJV in increasing EELV. However, both modes may provide adequate ventilation in the absence of airway obstruction and respiratory disease, except for HFJV at frequencies  $\geq 300 \text{ min}^{-1}$ . Further studies investigating the effects of frequency and ventilation mode when the airway is obstructed are warranted.

## Supplementary material

Supplementary material is available at *British Journal of Anaesthesia* online.

## Acknowledgements

The authors thank Agneta Roneus, Karin Fagerbrink, and Maria Lundqvist for their skilled technical assistance in the laboratory and Marcus Thuresson (Statisticon AB, Uppsala, Sweden) for assistance with the statistical analyses.

## Declaration of interest

A.A. is one of the inventors of opto-electronic plethysmography. The patents are owned by the Politecnico di Milano (Milan, Italy) and licensed to BTS Spa Company.

## Funding

This work was supported by grants from Uppsala University Hospital, the Tore Nilsson Research Foundation, the Swedish Heart Lung Foundation, Swedish Medical Research Council (grant number 5315), and Politecnico di Milano-Instituto Italiano di Tecnologia (IIT) unit.

## References

- 1 Sanders RD. Two ventilating attachments for bronchoscopes. *Del Med J* 1967; **39**: 170–5
- 2 Spoerel WE, Greenway RE. Technique of ventilation during endolaryngeal surgery under general anaesthesia. *Can Anaesth Soc J* 1973; **20**: 369–77
- 3 Baraka A. Oxygen-jet ventilation during tracheal reconstruction in patients with tracheal stenosis. *Anesth Analg* 1977; **56**: 429–32
- 4 El-Baz N, Jensik R, Faber LP, Faro RS. One-lung high-frequency ventilation for tracheoplasty and bronchoplasty: a new technique. *Ann Thorac Surg* 1982; **34**: 564–71
- 5 Rogers RC, Gibbons J, Cosgrove J, Coppel DL. High-frequency jet ventilation for tracheal surgery. *Anaesthesia* 1985; **40**: 32–6
- 6 Takahashi H, Takezawa J, Nishijima MK, et al. Effects of driving pressure and respiratory rate on airway pressure and PaCO<sub>2</sub> in rabbits during high-frequency jet ventilation. *Crit Care Med* 1985; **13**: 728–32
- 7 Biro P, Eyrich G, Rohling RG. The efficiency of CO<sub>2</sub> elimination during high-frequency jet ventilation for laryngeal microsurgery. *Anesth Analg* 1998; **87**: 180–4
- 8 Biro P, Layer M, Becker HD, et al. Influence of airway-occluding instruments on airway pressure during jet ventilation for rigid bronchoscopy. *Br J Anaesth* 2000; **85**: 462–5
- 9 Aloy A, Schachner M, Spiss CK, Cancura W. Tube-free translaryngeal superposed jet ventilation. *Anaesthesist* 1990; **39**: 493–8
- 10 Bacher A, Pichler K, Aloy A. Supraglottic combined frequency jet ventilation versus subglottic monofrequent jet ventilation in patients undergoing microlaryngeal surgery. *Anesth Analg* 2000; **90**: 460–5
- 11 Kraincuk P, Kormoczi G, Prokop M, Ihra G, Aloy A. Alveolar recruitment of atelectasis under combined high-frequency jet ventilation: a computed tomography study. *Intensive Care Med* 2003; **29**: 1265–72
- 12 Ng A, Russell WC, Harvey N, Thompson JP. Comparing methods of administering high-frequency jet ventilation in a model of laryngotracheal stenosis. *Anesth Analg* 2002; **95**: 764–9, table of contents
- 13 Buczkowski PW, Fombon FN, Lin ES, Russell WC, Thompson JP. Air entrainment during high-frequency jet ventilation in a model of upper tracheal stenosis. *Br J Anaesth* 2007; **99**: 891–7
- 14 Cala SJ, Kenyon CM, Ferrigno G, et al. Chest wall and lung volume estimation by optical reflectance motion analysis. *J Appl Physiol* 1996; **81**: 2680–9
- 15 Aliverti A, Dellaca R, Pelosi P, Chiumello D, Pedotti A, Gattinoni L. Optoelectronic plethysmography in intensive care patients. *Am J Respir Crit Care Med* 2000; **161**: 1546–52
- 16 Dellaca RL, Aliverti A, Pelosi P, et al. Estimation of end-expiratory lung volume variations by optoelectronic plethysmography. *Crit Care Med* 2001; **29**: 1807–11
- 17 Aliverti A, Kostic P, Lo Mauro A, et al. Effects of propofol anaesthesia on thoraco-abdominal volume variations during spontaneous breathing and mechanical ventilation. *Acta Anaesthesiol Scand* 2011; **55**: 588–96
- 18 Aliverti A, Carlesso E, Dellacà R, et al. Chest wall mechanics during pressure support ventilation. *Crit Care* 2006; **10**: R54
- 19 Rezaie-Majd A. Superimposed high-frequency jet ventilation (SHFJV) for endoscopic laryngotracheal surgery in more than 1500 patients. *Br J Anaesth* 2006; **96**: 650–9
- 20 Rouby JJ, Simonneau G, Benhamou D, et al. Factors influencing pulmonary volumes and CO<sub>2</sub> elimination during high-frequency jet ventilation. *Anesthesiology* 1985; **63**: 473–82
- 21 Leiter R, Aliverti A, Priori R, et al. Comparison of superimposed high-frequency jet ventilation with conventional jet ventilation for laryngeal surgery. *Br J Anaesth* 2012; **108**: 690–7
- 22 Chang HK. Mechanisms of gas transport during ventilation by high-frequency oscillation. *J Appl Physiol* 1984; **56**: 553–63
- 23 Fredberg JJ. Augmented diffusion in the airways can support pulmonary gas exchange. *J Appl Physiol* 1980; **49**: 232–8
- 24 Korvenranta H, Carlo WA, Goldthwait DA Jr, Fanaroff AA. Carbon dioxide elimination during high-frequency jet ventilation. *J Pediatr* 1987; **111**: 107–13
- 25 Rossing TH, Slutsky AS, Lehr JL, Drinker PA, Kamm R, Drazen JM. Tidal volume and frequency dependence of carbon dioxide elimination by high-frequency ventilation. *N Engl J Med* 1981; **305**: 1375–9
- 26 Rouby JJ, Fusciardi J, Bourgain JL, Viars P. High-frequency jet ventilation in postoperative respiratory failure: determinants of oxygenation. *Anesthesiology* 1983; **59**: 281–7
- 27 Biro P, Wiedemann K. Jet ventilation and anaesthesia for diagnostic and therapeutic interventions of the airway. *Anaesthesist* 1999; **48**: 669–85



- 28 Lin ES, Jones MJ, Mottram SD, Smith BE, Smith G. Relationship between resonance and gas exchange during high frequency jet ventilation. *Br J Anaesth* 1990; **64**: 453–9
- 29 Holmdahl MH. Pulmonary uptake of oxygen, acid–base metabolism, and circulation during prolonged apnoea. *Acta Chir Scand Suppl* 1956; **212**: 1–128
- 30 Nielsen ND, Andersen G, Kjaergaard B, Staerkind ME, Larsson A. Alveolar accumulation/concentration of nitrogen during apneic oxygenation with arteriovenous carbon dioxide removal. *ASAIO J* 2010; **56**: 30–4
- 31 Standiford TJ, Morganroth ML. High-frequency ventilation. *Chest* 1989; **96**: 1380–9

*Handling editor: J. P. Thompson*